

## Supporting information

### Alcohol-Soluble Conjugated Polymers Enable Highly Efficient and Stable Organic Solar Cells Through a Main-Chain Modulation Strategy

*Haiyang Zhao<sup>†</sup>, Zixin Huang<sup>†</sup>, Zhibin Li, Haoran Tang\*, Yuanqing Bai, Hui Li, Chunchen Liu, Kai Zhang and Fei Huang\**

H. Zhao, Z. Huang, Z. Li, H. Tang, Y. Bai, H. Li, C. Liu, K. Zhang, F. Huang

Institute of Polymer Optoelectronic Materials and Devices, State Key Laboratory of Luminescent Materials and Devices, Guangdong Basic Research Center of Excellence for Energy & Information Polymer Materials, South China University of Technology, Guangzhou 510641, P. R. China

E-mail: mstanghaoran@scut.edu.cn; msfhuang@scut.edu.cn

*<sup>†</sup> These two authors contributed equally to this work*

## Contents

- 1. Materials and General Procedures**
- 2. Devices Fabrication**
- 3. Measurements and Characterizations**
- 4. Synthetic Procedures and Characterizations**
- 5. Additional Figures and NMR Spectra**
- 6. References**

## 1. Materials and General Procedures

All the solvents and chemical reagents were obtained commercially from Energy Chemical Co., J&K Co., Bide Pharmatech Co., etc. and were used without further purification, unless otherwise stated. PM6, D18, Y6, and L8-BO were purchased from Solarmer Materials Inc. PFN-Br and DTC11 were purchased from Dongguan Volt-Amp Optoelectronics Technology Co. Ltd. PEDOT:PSS (Clevios P VP Al 4083) was purchased from Heraeus. NDA-2Br was synthesized by the previous reference.<sup>[1]</sup>

The <sup>1</sup>H NMR and <sup>13</sup>C NMR spectra were analyzed on a Bruker AV-500 MHz spectrometer with deuterated chloroform (CDCl<sub>3</sub>) used in the test. UV-vis absorption spectra were recorded on a SHIMADZU UV-3600 spectrophotometer. Cyclic voltammetry (CV) was measured by CHI660E electrochemical workstation with a saturated calomel reference electrode, platinum wire counter electrode, glass carbon working electrode and 0.1 M tetrabutylammonium hexafluorophosphate (n-Bu<sub>4</sub>NPF<sub>6</sub>) as electrolyte. TGA measurements were conducted on a Netzsch TG209 apparatus at a heating rate of 20 °C min<sup>-1</sup> under nitrogen atmosphere. DSC measurements were performed on a NETZSCH DSC200 apparatus under nitrogen atmosphere with a heating/cooling rate of 20 °C min<sup>-1</sup>. The gel permeation chromatography (GPC) measurements were conducted on Agilent-1260 apparatus. Ultraviolet Photoelectron Spectroscopy (UPS) spectra were performed on Thermo Scientific Escalab 250XI apparatus. Scanning Kelvin Probe Microscopy (KPM) measurements were conducted by UHV SKP Measurement (KP Technology Ltd). The atomic force microscopy (AFM) measurements were measured by Digital Instrumental DI Multimode Nanoscope III in a tapping mode. The grazing incidence wide-angle X-ray scattering (GIWAXS) measurements were performed at Xenocs, France, Xeuss 2.0. Contact angle measurements were performed using a water or ethylene glycol contact angle measurement system (OCA40 Micro).

## 2. Devices Fabrication

The OSC devices were fabricated with conventional structures of ITO/PEDOT:PSS/Active layer/Cathode interlayer materials/Ag. The ITO substrates were cleaned by detergent, deionized water and isopropanol under sonication. After being treated with oxygen plasma for about 5 min, PEDOT:PSS (Clevios P VP Al 4083) layer (~15-20 nm) was spin-coated on the top of ITO and annealed in the air at 150 °C for 15 min. Then, the active layer (D:A=1:1.2, 4 mg mL<sup>-1</sup>:4.8

mg mL<sup>-1</sup>) was dissolved in carbon disulfide and o-xylene (vol.ratio=0.5:0.5) mixed solution, and stirred at 65 °C for 1.5 h in glove box. Later, the active layer with a thickness of ~100 nm was spin-coated on the ITO/PEDOT:PSS substrate and the obtained device was annealed at 85 °C for 5 min. Subsequently, PNDITphN solution (0.75 mg mL<sup>-1</sup> in methanol with 1% acetic acid in volume) or PNDITphN-Br solution (1 mg mL<sup>-1</sup> in methanol) was spin-coated on the top of the active layer to form a ~10 nm cathode interlayer. Finally, a 100 nm Ag layer was deposited by thermal vacuum evaporation under 10<sup>-6</sup> mbar and obtained 0.0516 cm<sup>2</sup> active area device. Physical aperture with the area of 0.04 cm<sup>2</sup> was capped on OSCs for efficiency test.

### 3. Measurements and Characterizations

*J-V, EQE measurements:* The current density voltage (*J-V*) characteristics were measured under a computer-controlled Keithley 2400 source meter under 1 sun, AM 1.5G solar simulator (Taiwan, Enlitech SS-F5). The light intensity was calibrated by a standard silicon solar cell (certified by China General Certification Center) before the test, giving a value of 100 mW cm<sup>-2</sup> during the test of *J-V* characteristics. The external quantum efficiency (EQE) spectra were recorded with a QE-R measurement system (Enlitech, QE-R3011, Taiwan).

*Space-charge-limited-current (SCLC) measurement:* The architecture of electron-only device was ITO/ZnO/DTC11/CIMs/Ag. The mobility was determined by fitting the dark current to the model of a single-carrier SCLC, which is described by equation S1.

$$J = \frac{9}{8} \epsilon_0 \epsilon_r \mu_h \frac{V^2}{d^3} \quad (S1)$$

where *J* is the current density,  $\mu$  is the zero-field mobility,  $\epsilon_0$  is the permittivity of free space,  $\epsilon_r$  is the relative permittivity of the material, *d* is the thickness of the active layers, and *V* is the effective voltage. The effective voltage was calculated by the equation:  $V = V_{\text{appl}} - V_{\text{bi}} - V_s$ , where  $V_{\text{appl}}$  is the applied voltage,  $V_{\text{bi}}$  is the built-in voltage, and  $V_s$  is the voltage drop of the substrate series resistance. The electron mobility can be calculated from the slope of the  $J^{1/2}$ -*V* curves.

*Transient photocurrent (TPC) and transient photovoltage (TPV) measurements:* The TPC and TPV of the OSCs was measured by applying 530 nm laser pulses with a pulse width of 120 fs and a low pulse energy to the short-circuited devices in the dark. The laser pulses were generated from an optical parametric amplifier (TOPAS-Prime) pumped by a mode-locked Ti:sapphire oscillator-seeded regenerative amplifier with a pulse energy of 1.3 mJ at 800 nm

and a repetition rate of 1 kHz (Spectra Physics Spitfire Ace). The photocurrent produced a transient voltage signal on a 50  $\Omega$  resistor, which was recorded by a S3 Tektronix TDS3052C oscilloscope. The TPV was testing under the open-circuit condition to explore the photovoltage decay. The photovoltage decay kinetics of all devices follow a mono-exponential decay:  $\delta V = A \exp(-t/\tau)$  where  $t$  is the time, and  $\tau$  is the charge carrier lifetime.

Mott-Schottky, TPV, CE and Electrochemical Impedance Spectroscopy measurements: These measurements were performed by the all-in-one characterization platform Paios developed and commercialized by Fluxim AG, Switzerland. Mott-Schottky measurement was tested within the voltage range from -3 V to 2 V under dark condition. And the Mott-Schottky equation is described as Equation S2.

$$\frac{1}{C^2} = \frac{2(V_{bi} - V)}{A^2 q \epsilon_0 \epsilon_r N} \quad (S2)$$

Where  $C$  is the capacitance value,  $V$  is the applied voltage,  $A$  is the device area,  $q$  is the elementary charge,  $\epsilon_r$  is the relative dielectric constant,  $\epsilon_0$  is the vacuum permit-tivity, and  $N$  is the charge carrier density. TPV measurement was measured under open-circuit voltage condition, and variable bias light intensities led to the change of  $V_{OC}$ . As for CE measurement, firstly, devices were at open circuit and under light, then the light was turned off, the voltage was set to zero or taken to short-circuit condition within a few hundred nanoseconds to extract charges. The impedance characteristics were measured with the frequency measurement range of 1 Hz to 10 MHz under dark conditions.

#### 4. Synthetic procedures and characterizations

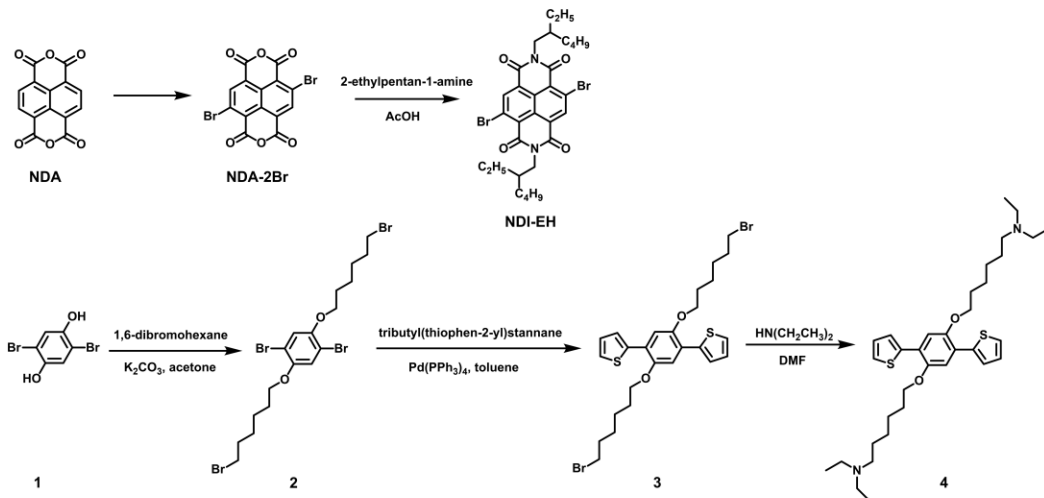


Figure S1. Monomer synthesis routes.

**4,9-dibromo-2,7-bis(2-ethylhexyl)benzo[lmn][3,8]phenanthroline-1,3,6,8(2H,7H)-tetraone (NDI-EH)**

NDA-2Br (2.0780 g, 4.9 mmol) was suspended in 50 ml acetic acid under nitrogen atmosphere and 2-ethyl-hexyl amine (1.8914g, 3 eq.) was added to the flask by syringe. The reaction was stirred at 120 °C for 3 hours. After cooling down to room temperature, the mixture was poured into ice water. The resulting precipitate was collected by suction filtration and the filtrate was purified by silica gel column chromatography (PE/DCM= 1/1). <sup>1</sup>H NMR (500 MHz, Chloroform-*d*) δ 9.00 (s, 2H), 4.16 (t, *J* = 7.8 Hz, 4H), 1.94 (dt, *J* = 12.8, 6.5 Hz, 2H), 1.44 – 1.24 (m, 16H), 0.91 (dt, *J* = 25.1, 7.2 Hz, 12H). <sup>13</sup>C NMR (101 MHz, CDCl<sub>3</sub>) δ 161.24, 161.08, 139.20, 128.40, 127.79, 125.31, 124.10, 45.16, 37.77, 30.63, 28.54, 23.98, 23.08, 14.09, 10.58.

**1,4-dibromo-2,5-bis((6-bromohexyl)oxy)benzene (compound 2)**

Compound 1 2,5-dibromobenzene-1,4-diol (10.9990 g, 41.1 mmol) and potassium carbonate (22.6976 g, 4 eq.) were dissolved in acetone under nitrogen atmosphere and heated to 60 °C for 1 hour. 1,6-dibromohexane (60.1094 g, 6 eq.) was injected and the mixture was stirred for 18 hours. The solvent was removed under vacuum using rotary evaporation. The residue was purified by silica gel column chromatography by using petroleum ether (PE): dichloromethane (DCM) (3/1) as eluent. Recrystallization using DCM/PE afforded the target compound as white solid (10.2510 g, yield 42.0%). <sup>1</sup>H NMR (500 MHz, Chloroform-*d*) δ 7.08 (s, 2H), 3.96 (t, *J* = 6.3 Hz, 4H), 3.43 (t, *J* = 6.8 Hz, 4H), 1.91 (p, *J* = 6.9 Hz, 4H), 1.82 (q, *J* = 6.6 Hz, 4H), 1.53 (dd, *J* = 6.9, 3.3 Hz, 8H). <sup>13</sup>C NMR (101 MHz, CDCl<sub>3</sub>) δ 150.08, 118.52, 111.19, 70.05, 33.79, 32.67, 28.95, 27.85, 25.22.

**2,2'-(2,5-bis((6-bromohexyl)oxy)-1,4-phenylene) dithiophene (compound 3)**

1,4-dibromo-2,5-bis((6-bromohexyl)oxy)benzene (535.2 mg, 0.9 mmol) and tributyl(thiophen-2-yl) stannane (706.1 mg, 3 eq.) were dissolved in 5 ml dry toluene and the mixture was purged by nitrogen twice. Under N<sub>2</sub> atmosphere, Pd(PPh<sub>3</sub>)<sub>4</sub> (104.1 mg, 0.1 eq) was added carefully to the flask and the reaction was stirred at 120 °C overnight. After removal of the solvent, the crude product was purified via column chromatography (PE/DCM= 3/1). Recrystallization using DCM/PE afforded the target compound as pale yellow solid (380.5 mg, yield 70.3 %). <sup>1</sup>H NMR (500 MHz, Chloroform-*d*) δ 7.52 (dd, *J* = 3.7, 1.1 Hz, 2H), 7.35 (dd, *J* = 5.1, 1.0 Hz, 2H), 7.25 (s, 2H), 7.10 (dd, *J* = 5.1, 3.7 Hz, 2H), 4.09 (t, *J* = 6.4 Hz, 4H), 3.42 (t,

$J = 6.8$  Hz, 4H), 1.91 (h,  $J = 6.5$  Hz, 8H), 1.60 – 1.54 (m, 8H).  $^{13}\text{C}$  NMR (101 MHz,  $\text{CDCl}_3$ )  $\delta$  149.22, 139.18, 126.75, 125.80, 125.21, 123.06, 112.92, 69.47, 33.83, 32.67, 29.25, 27.92, 25.47.

**6,6'-((2,5-di(thiophen-2-yl)-1,4-phenylene)bis(oxy))bis(N,N-diethylhexan-1-amine)**  
(compound 4)

2,2'-(2,5-bis((6-bromohexyl)oxy)-1,4-phenylene) dithiophene (1.9423 g, 3.2 mmol) was dissolved in 10 ml dry DMF and the mixture was purged by nitrogen twice. Diethylamine (6 ml) was added through syringe under nitrogen atmosphere and the reaction was stirred at 80 °C overnight. The solvent was removed under vacuum using rotary evaporation. The crude product was purified via column chromatography (PE/DCM/TEA= 15/15/1) to give the target compound as yellow solid (163.3 mg, yield 81.1%).  $^1\text{H}$  NMR (500 MHz, Chloroform- $d$ )  $\delta$  7.52 (d,  $J = 3.6$  Hz, 2H), 7.34 (d,  $J = 4.6$  Hz, 2H), 7.25 (s, 2H), 7.09 (dd,  $J = 5.0, 3.8$  Hz, 2H), 4.08 (t,  $J = 6.5$  Hz, 4H), 2.64 – 2.51 (m, 8H), 2.50 – 2.40 (m, 4H), 1.91 (dt,  $J = 14.4, 6.6$  Hz, 4H), 1.54 (dp,  $J = 20.3, 7.6$  Hz, 8H), 1.39 (h,  $J = 7.5$  Hz, 4H), 1.05 (t,  $J = 7.0$  Hz, 12H).  $^{13}\text{C}$  NMR (101 MHz,  $\text{CDCl}_3$ )  $\delta$  149.24, 139.27, 126.73, 125.71, 125.17, 123.02, 112.89, 69.65, 52.89, 46.90, 29.42, 27.49, 26.89, 26.26, 11.60.

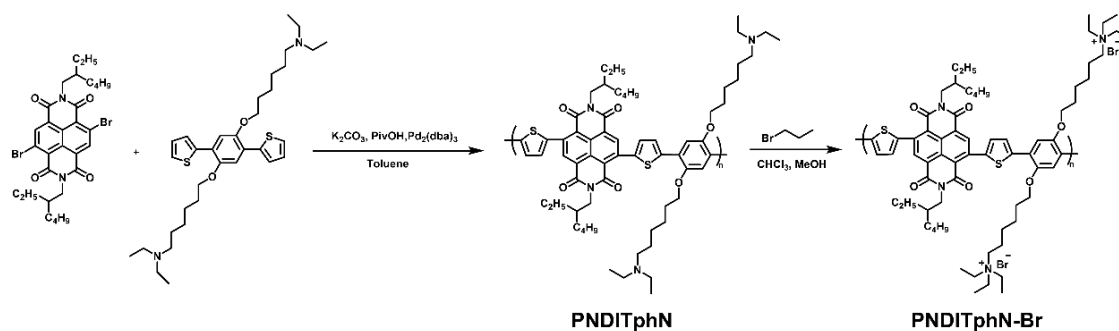


**Figure S2.** Polymer synthesis routes.

**Polymerization of PNDITphN**

NDI-EH (58.5 mg, 0.1 mmol), 4 (52.8 mg, 0.1 mmol), potassium carbonate (31.2 mg, 2.5 eq.), pivalic acid (9.2 mg, 1.0 eq.) and  $\text{Pd}_2(\text{dba})_3$  (1 mg) were combined in a 15 mL sealed tube and the mixture was purged by argon twice. Dry chlorobenzene (CB) (1.8 mL) was added under argon atmosphere. The reaction mixture was stirred at 90 °C for 72 h. After cooling down to room temperature, the reactant mixture was poured into MeOH (200 mL), forming of the dark green precipitate. The precipitate was filtered and successively extracted with methanol, acetone, hexane and chloroform by Soxhlet extraction. The chloroform fraction was

concentrated and precipitated into methanol. The precipitate was collected and dried under vacuum overnight. **PNDITphN**: 82.0 mg, yield 84.7%. ( $M_n = 7.7$  kDa,  $M_w = 22.8$  kDa, PDI = 2.97).

### Synthesis of PNDITphN-Br

PNDITphN (22.5 mg) was dissolved in 1 ml  $\text{CHCl}_3$ , followed by the addition of 1 mL of bromoethane. The mixture was stirred at 50 °C for 4 days, once some precipitates appeared, some methanol was added to dissolve them. Then the solvent was removed under reduced pressure, and the crude product was dissolved in methanol (10 ml). The solution was filtered with a 0.45 $\mu\text{m}$  PTFE filter, concentrated and precipitated from ethyl acetate. The solid was collected and dried under vacuum overnight. **PNDITphN-Br**: 24.4 mg, yield 90.1%.

## 5. Additional Figures and NMR Spectra

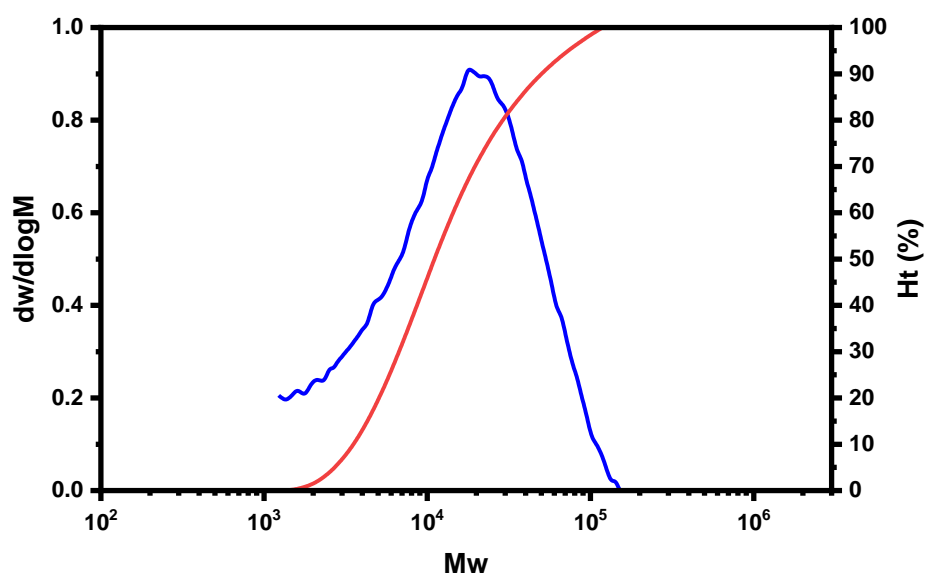


**Figure S3.** The GPC spectra of PNDITphN using  $\text{CHCl}_3$  as mobile phases.

**Table S1.** Molecular weights of PNDITphN and PNDITphN-Br.

	$M_n$ (KDa)	$M_w$ (KDa)	PDI
PNDITphN	7.7	22.8	2.97

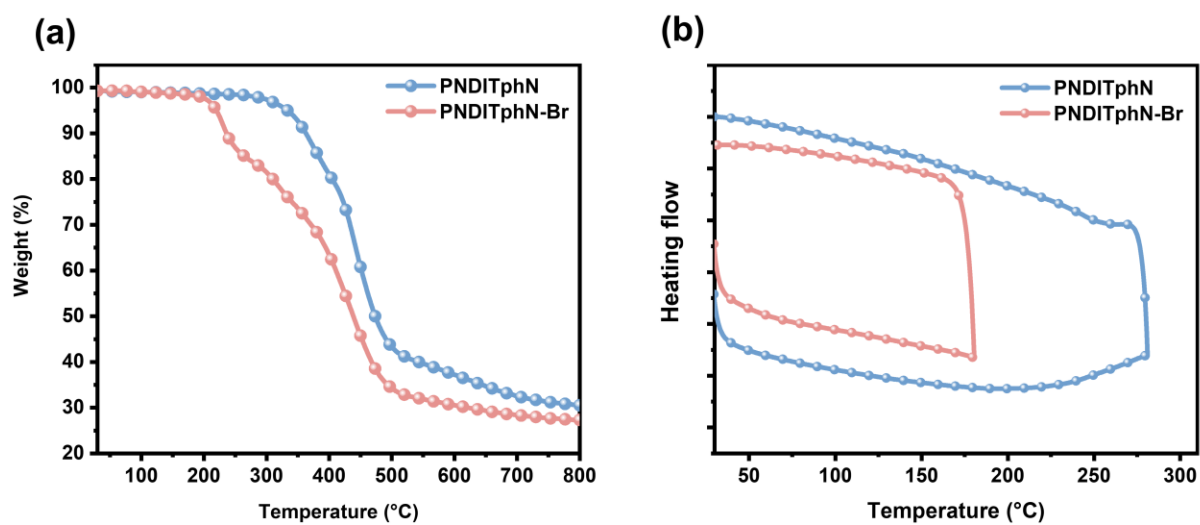


**Figure S4.** a) Thermogravimetric curve of PNDITphN and PNDITphN-Br; b) Differential Scanning Calorimetry curve of PNDITphN and PNDITphN-Br.

**Table S2.** Decomposition temperature of PNDITphN and PNDITphN-Br.

	PNDITphN	PNDITphN-Br
$T_d$ (°C) <sup>a)</sup>	332	215

<sup>a)</sup> 5% weight loss temperature.

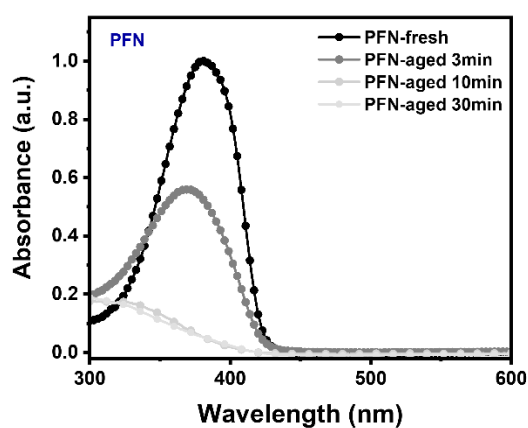


**Figure S5.** The time-dependent UV-vis absorption spectra of PFN.

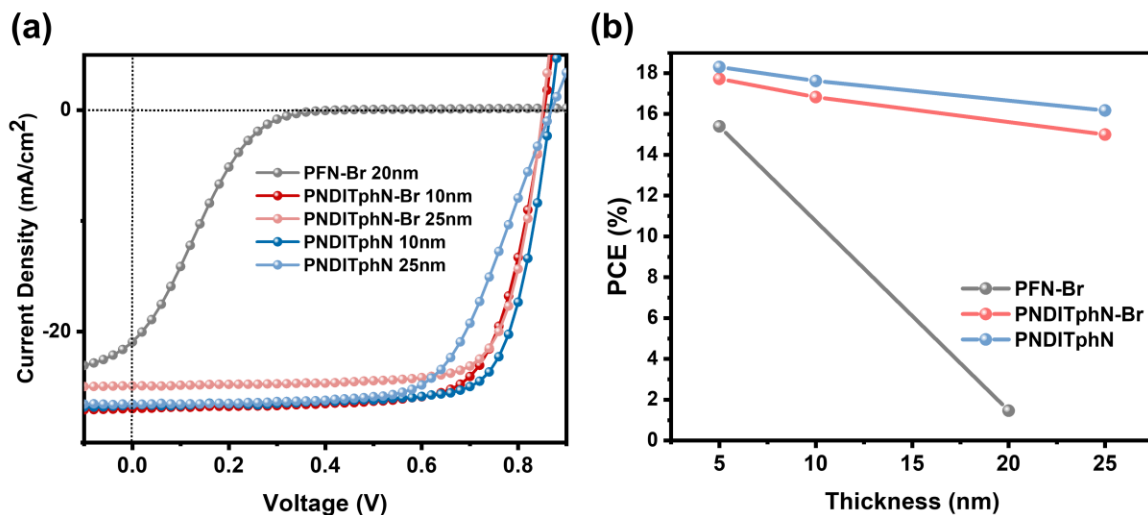


**Figure S6.** a) J–V curves of PNDITphN and PNDITphN-Br of various thicknesses with the active layer of D18:DTC11. b) Dependence of PCE on the film thickness.

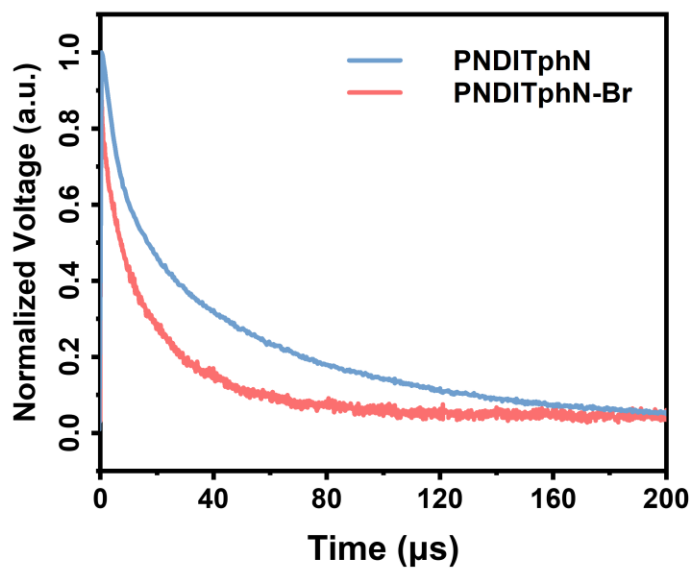


**Figure S7.** Normalized transient photovoltage traces of devices.

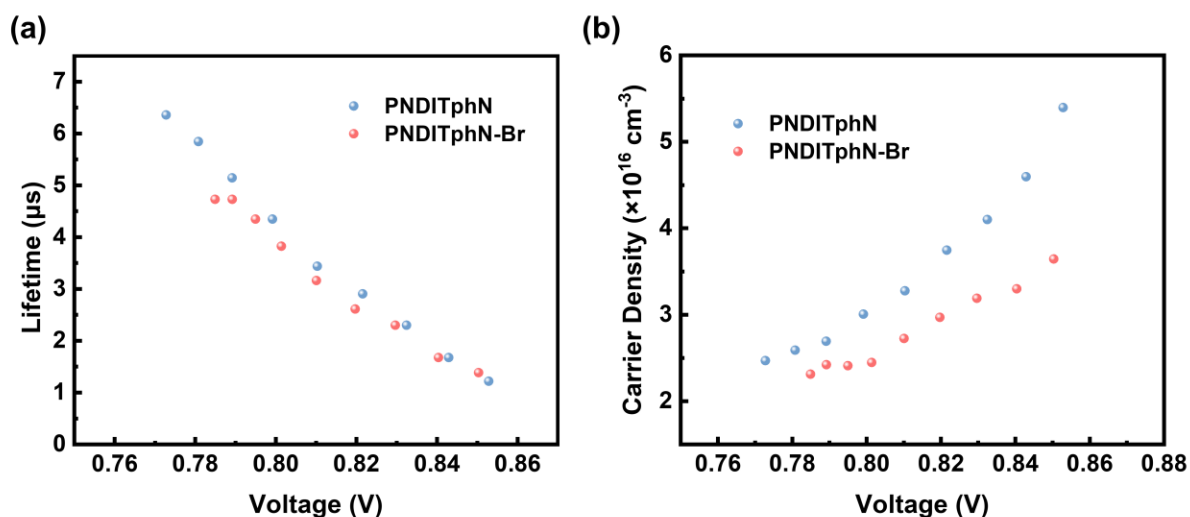


**Figure S8.** a) The carrier lifetime as a function of voltage under different bias light intensities; b) The extracted carrier density under different open circuit conditions.

**Table S3.** Fitting parameters for impedance spectra.

CIMs	$R_s$ ( $\Omega$ )	$R_{\text{bulk}}$ ( $\text{k}\Omega$ )	$C_{\text{bulk}}$ (nF)	$R_{\text{interface}}$ ( $\text{k}\Omega$ )	$C_{\text{interface}}$ (nF)
PNDITphN	8.22	12.4	1.83	80	1.6
PNDITphN-Br	9.44	21.9	3.35	113	2.45

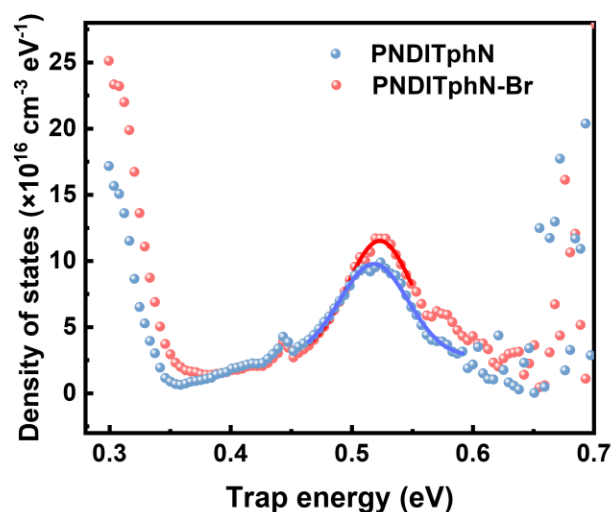


**Figure S9.** Trap density of states of devices based on PNDITphN and PNDITphN-Br

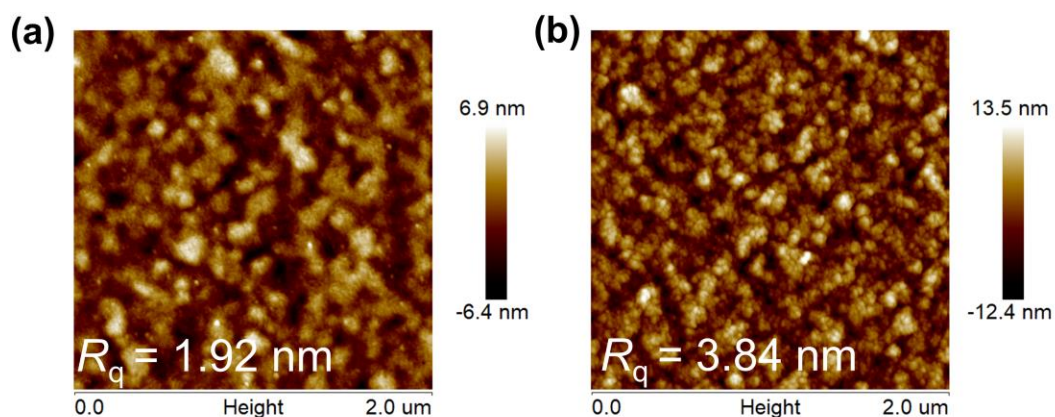


**Figure S10.** AFM height images of a) PNDITphN and b) PNDITphN-Br films

**Table S4.** Contact angles and surface energies of active layer, PNDITphN and PNDITphN-Br.

Surface	Contact angle		$\gamma$ (mN m <sup>-1</sup> )
	$\theta_{\text{H}_2\text{O}}$ (°)	$\theta_{\text{EG}}$ (°)	
Active layer	100.2	77.1	20.87
PNDITphN	85.9	66.1	23.73
PNDITphN-Br	66.7	50.4	35.45

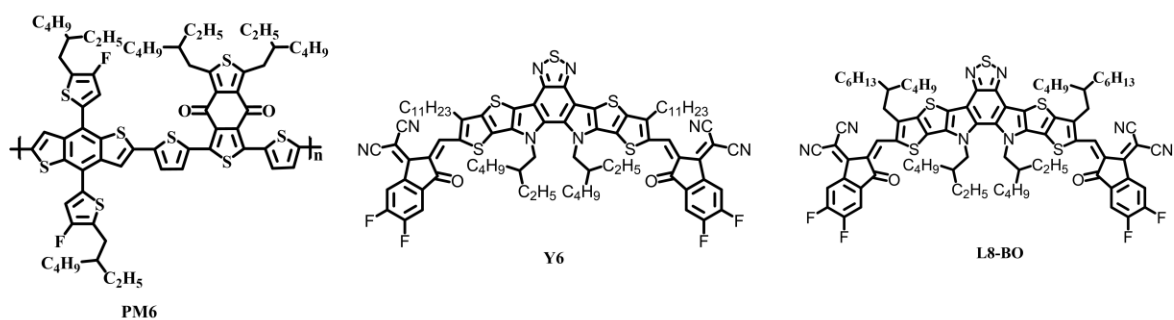


**Figure S11.** Molecular structures of active layer materials.

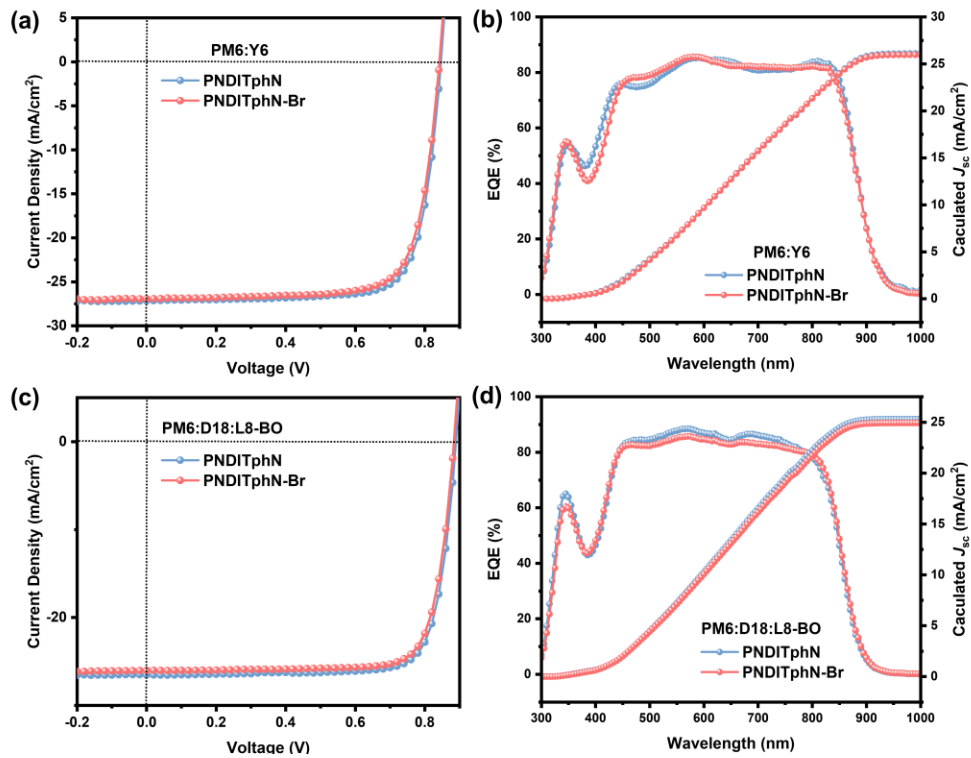


**Figure S12.** J–V curves and EQE curves of PNDITphN and PNDITphN-Br based devices with active layer of a) and b) PM6:Y6, c) and d) PM6:D18:L8-BO.

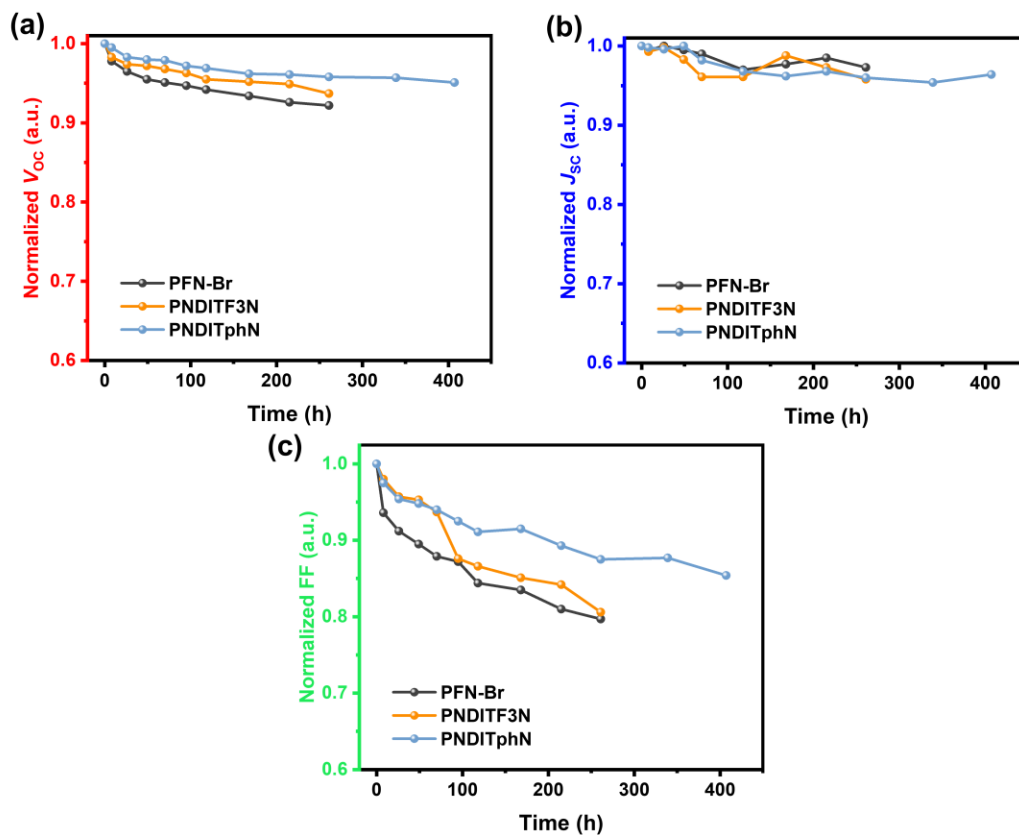


**Figure S13.** The trend of  $V_{OC}$ ,  $J_{SC}$  and FF as a function of light exposure time.

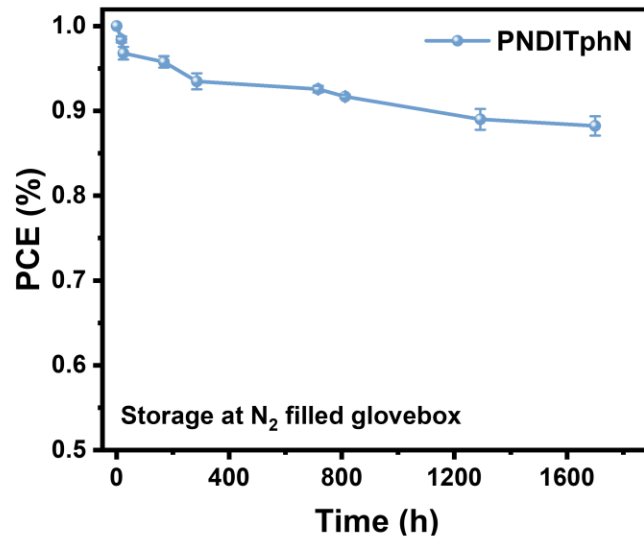


**Figure S14.** The PCE variation diagrams of devices based on polymer PNDITphN stored in glove box filled with N<sub>2</sub>

## Additional NMR Spectra

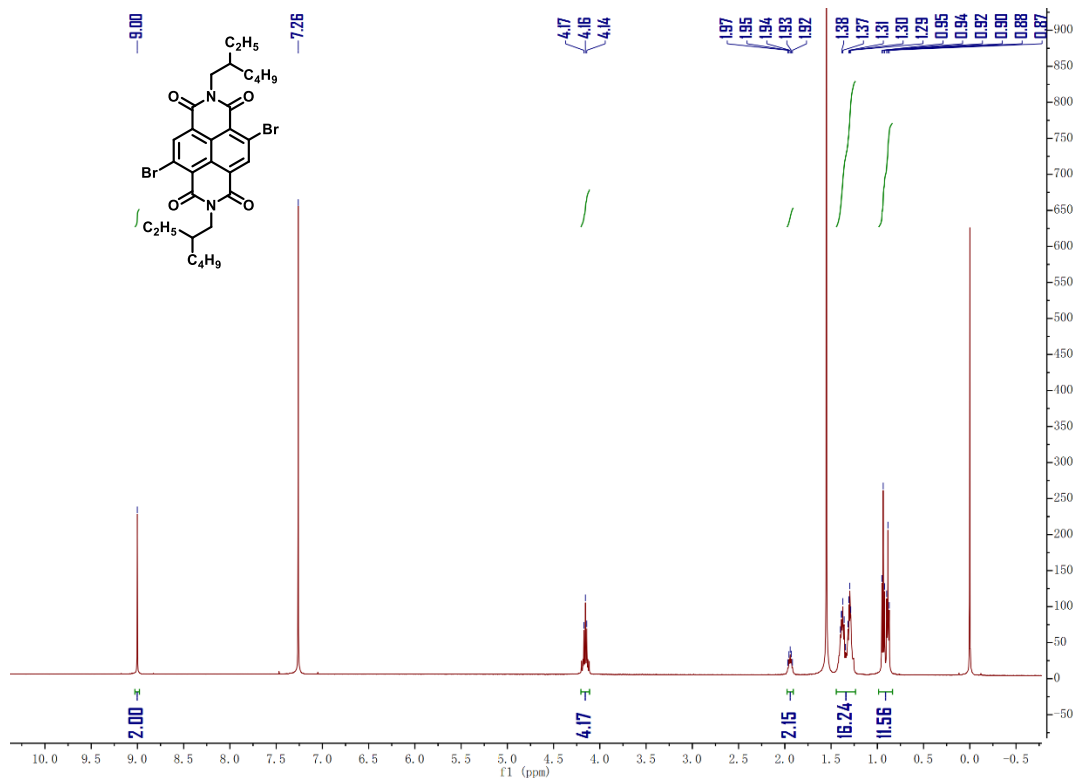


**Figure S15.** The  $^1\text{H}$  NMR spectrum of NDI-EH.

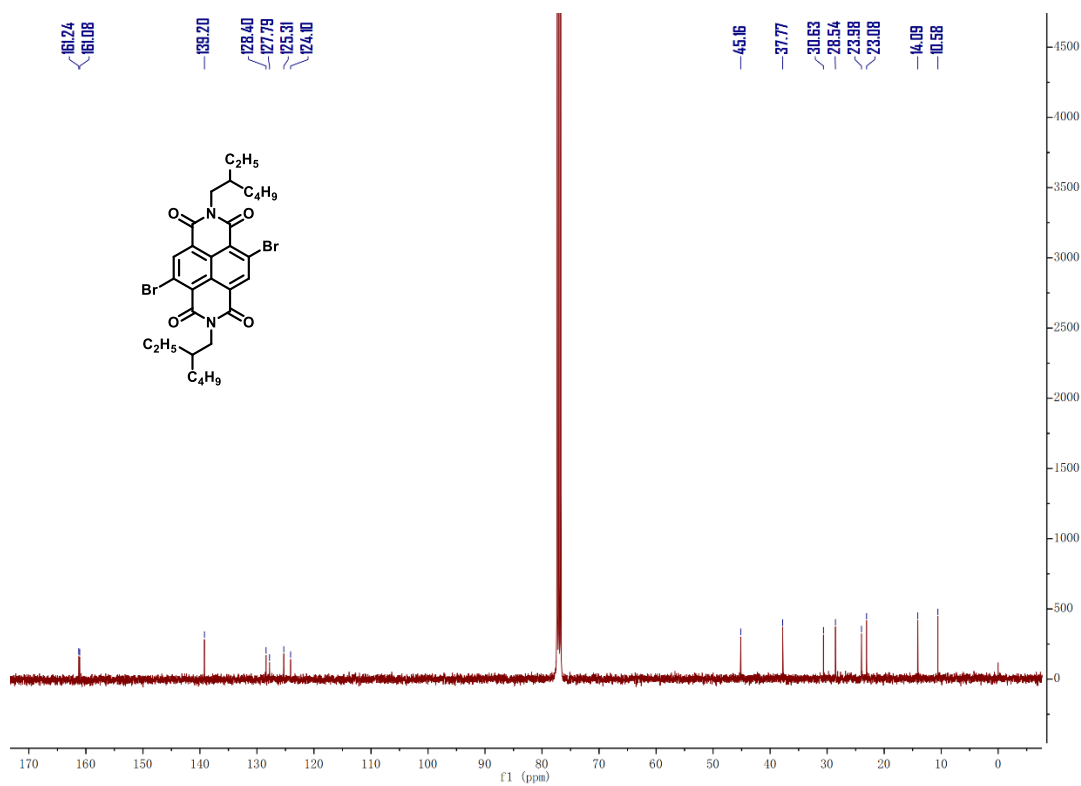


**Figure S16.** The  $^{13}\text{C}$  NMR spectrum of NDI-EH.

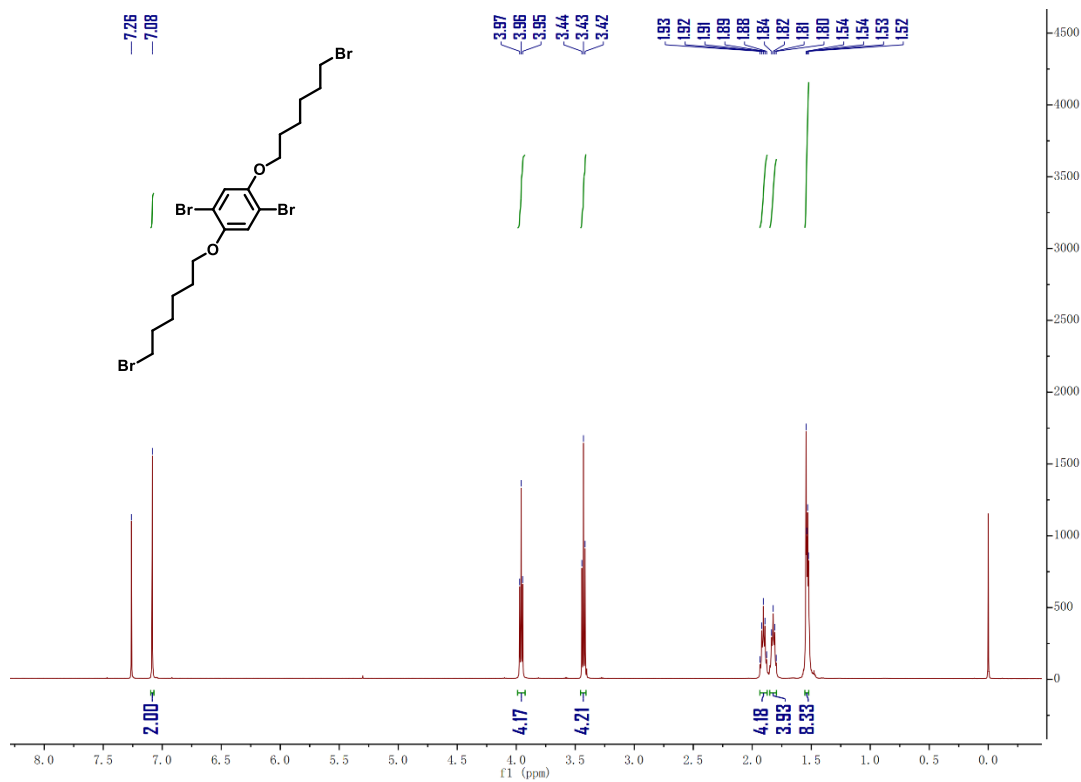


Figure S17. The  $^1\text{H}$ NMR spectrum of compound 2.

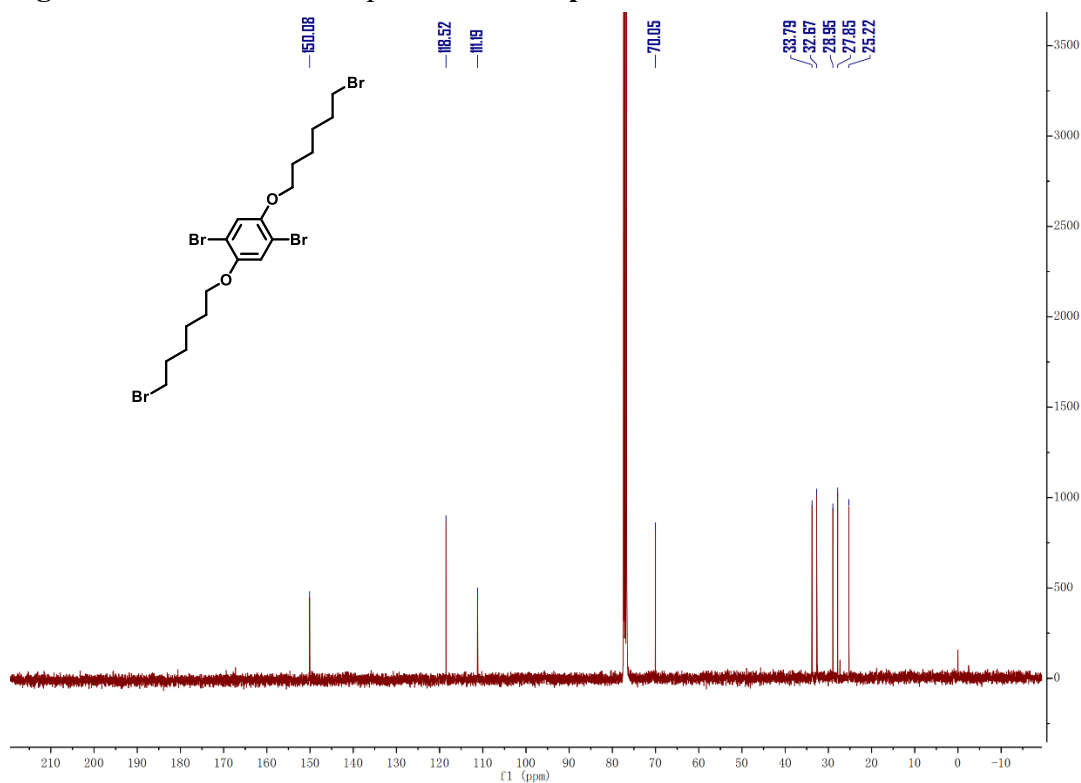


Figure S18. The  $^{13}\text{C}$  NMR spectrum of compound 2.

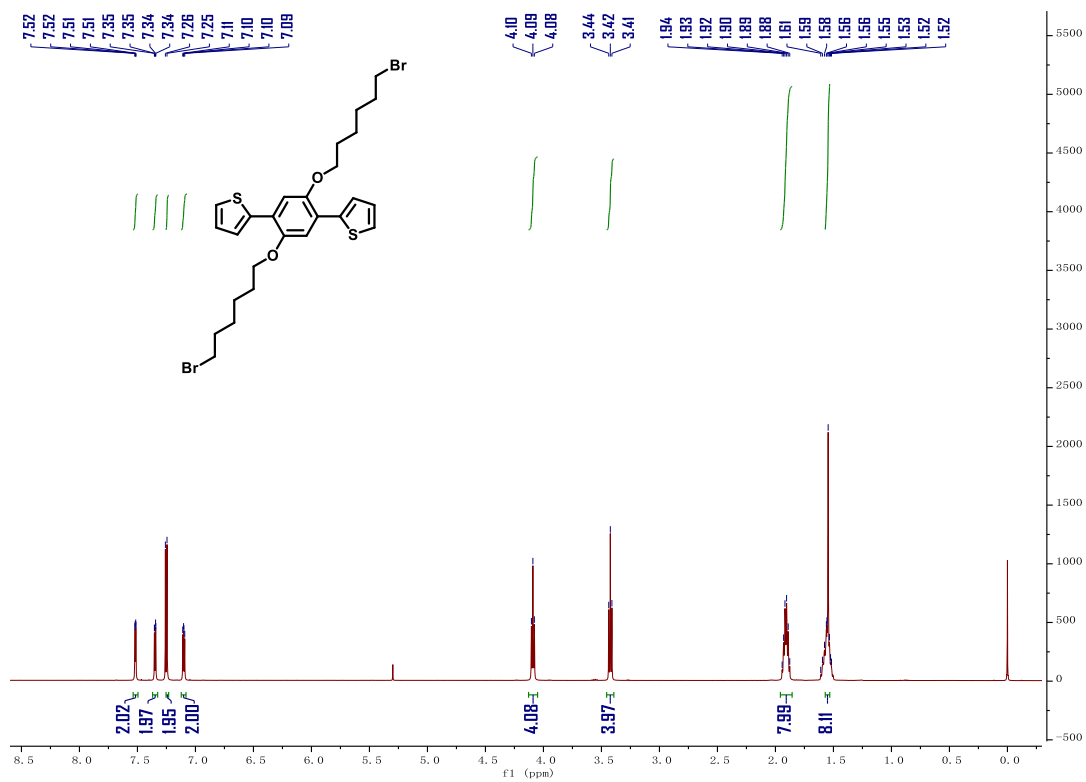


Figure S19. The <sup>1</sup>H NMR spectrum of compound 3.

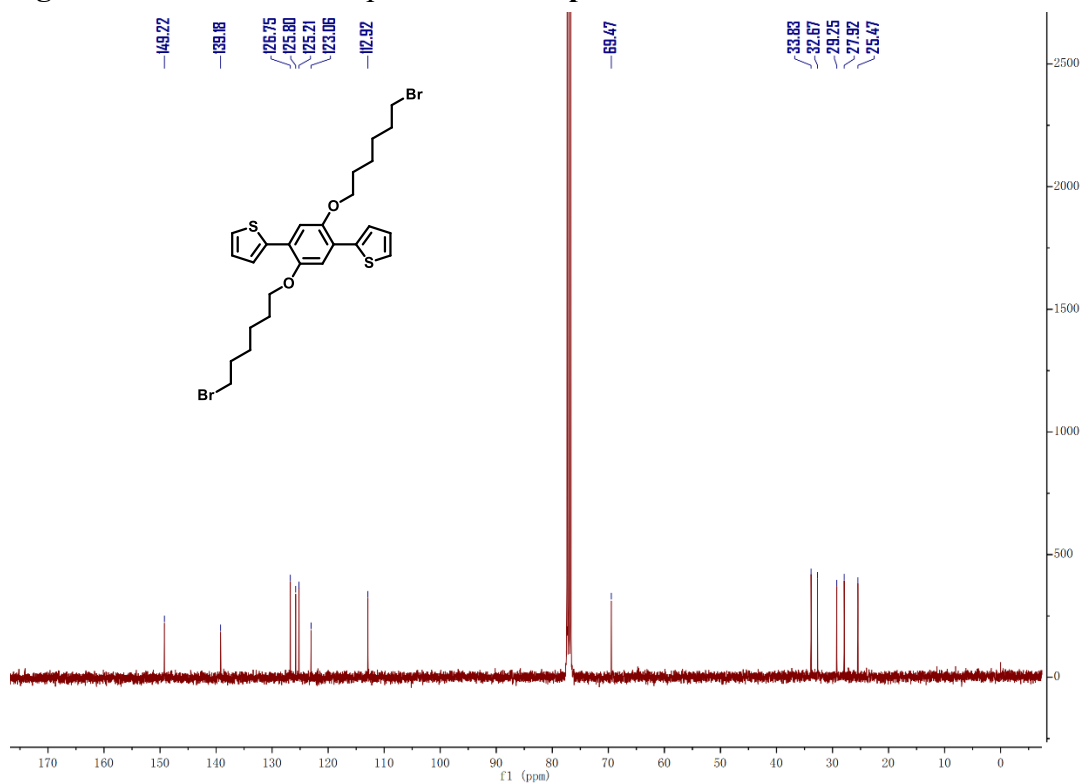


Figure S20. The <sup>13</sup>C NMR spectrum of compound 3.

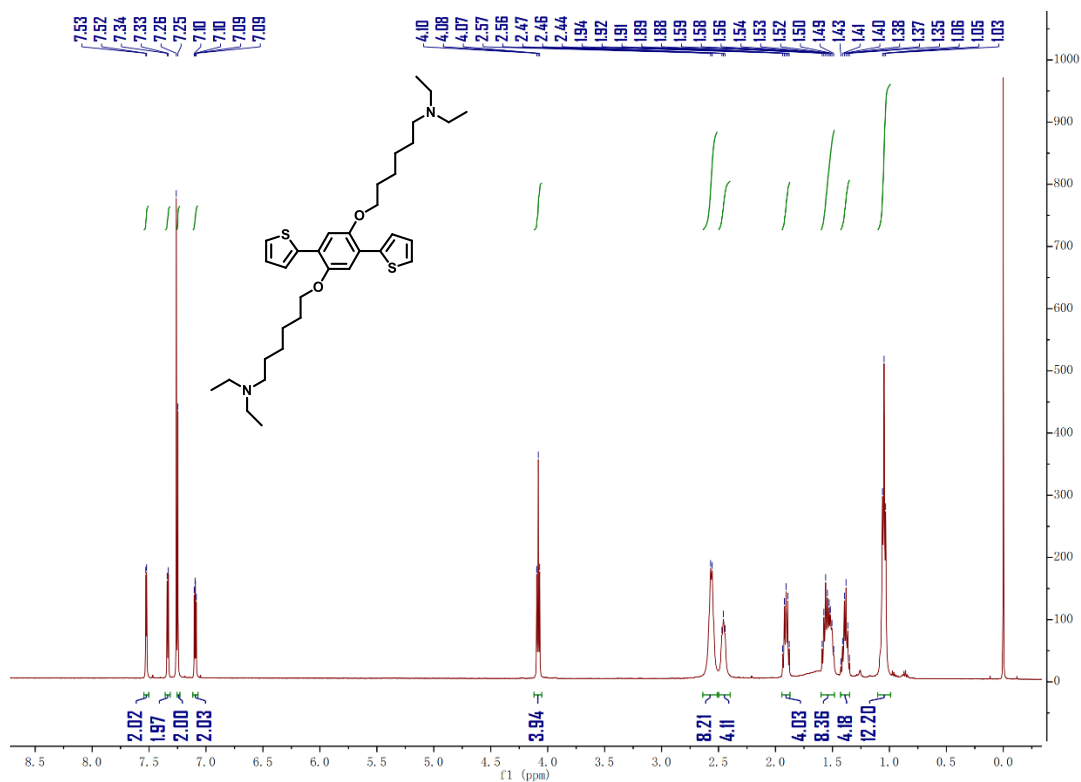


Figure S21. The  $^1\text{H}$ NMR spectrum of compound 4.

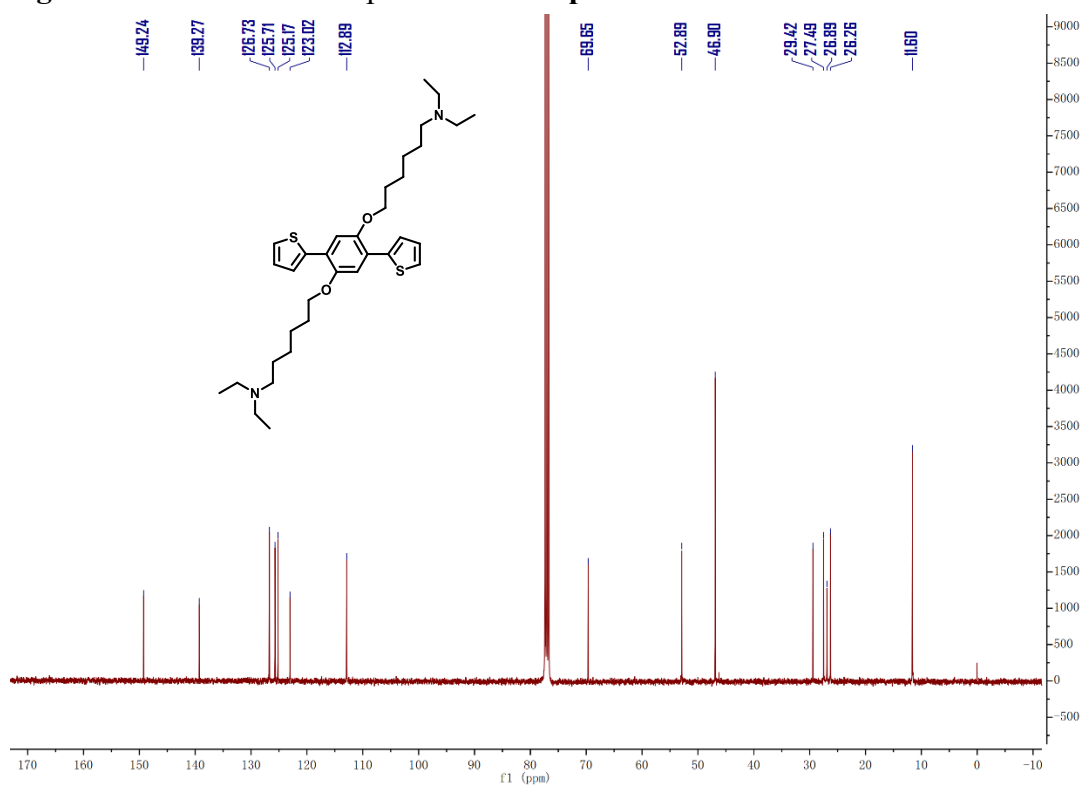


Figure S22. The  $^{13}\text{C}$ NMR spectrum of compound 4.

## 6. Reference

- [1] X. Guo, M. D. Watson, *Org. Lett.* **2008**, 10, 5333.